FUSION BONDING

Timo Mayer

Bachelor of Engineering
Mechanical Engineering

Department of Engineering
Macquarie University

November 2017

Supervisor: David Inglis

ACKNOWLEDGMENTS

I would like to acknowledge David, my supervisor who always had time for me and gave great feedback throughout the entire project, Aleksei, who was invaluable in helping me understand the chemistry associated with fusion bonding and Myna, who helped a lot during the testing of the samples.

STATEMENT OF CANDIDATE

I, Timo Mayer, declare that this report, submitted as part of the requirement for the award of Bachelor of Engineering in the Department of Mechanical Engineering, Macquarie University, is entirely my own work unless otherwise referenced or acknowledged. This document has not been submitted for qualification or assessment an any academic institution.

Student's Name: Timo Mayer

Student's Signature: 

Date: 6/11/2017

ABSTRACT

In nanofluidic applications and MEMS applications, two pieces of glass substrate often need to be bonded together permanently. In these cases, it can be difficult or cumbersome to use adhesives. Fusion bonding represents an alternative which can bond pieces of glass substrate to each other permanently without the hassle of adhesives or extra materials. In order to bond the glass substrates, it is necessary to clean them from any contamination. There are different ways of going about this and this project aims to investigate these different cleaning procedures in order to determine the optimal one.

Contents

List of Figures

List of Tables

Chapter 1

Introduction

1.1 Aim

As mentioned in the abstract, this project aims to find the optimal cleaning procedure for fusion bonding. "Optimal" here is subject to some interpretation as the main aim is to test samples bonded with different cleaning procedures in order to determine their strength and subsequently compare these strengths to find the strongest one. However, it may be the case that the strongest one is much more expensive, time consuming and dangerous to clean due to the chemicals used, in which case it would not be the 'optimal' clean, despite being the strongest one.

1.2 Motivation

Fusion Bonding has several advantages compared to using adhesives or other bonding methods. Firstly, it does not require any adhesive or voltage in order to bond, only cleanliness and heat. Secondly, once the glass substrate is bonded, the bond is irreversible, as the two pieces of glass substrate become part of each other on a molecular level. This means that when considering the application, no properties of adhesives or seperate materials (as in, for example frit bonding), need to be considered, and only the properties of the one material need to be considered. As well as this, finding the optimal fusion bond is useful due to it having many applications, the main ones being silicon on insulater material fabrication, power electronics, light emitting diodes with high brightness and micromechanical devices, and this is just for silicon direct wafer bonding [1]. The applications of bonding of other substrates such as Silicon Dioxide extend into nanofludics and MEMS (Microelectromechanical Systems), as well as others.

Other types of bonding for glass substrates include Anodic Bonding, where an applied voltage and heat is used to bond two glass substrates to silicon, plasma cleaning, where substrates' surfaces are cleaned by an Oxygen plasma, as well as several different types of adhesives such as super glue, epoxy and cyanoacrylate. Fusion bonding, which is in-

vestigated in this project, involves cleaning the surfaces of both pieces of glass substrate and subsequently bonding them at room temperature before heating to annealing temperatue in order to create an irreversible bond. Fusion bonding sets itself apart from these different bonding methods in many ways and this is elaborated on in the next section.

Chapter 2

Background & Theory

2.1 Bonding

2.1.1 Applications of Bonding

There are many different applications of bonding glass substrates. One common one is to bond glass wafers which have micro or nanofluidic channels etched into them in order to create seals. The creation of these microfluidic channels enable researchers to experiment with fluid flows on the micro- and nanoscale, in order to determine fluid behaviour, particle flow, boundary conditions and many other properties of different fluids [2]. For example, in [3], the authors use glass-glass fusion bonding in order to help them create nanochannels that are less than 40nm deep. In this application, fusion bonding has a clear advantage in that it allows for complete transperency at the bonded area, which is required in order to observe fluid behaviour under a microscope. Additionally, the technique of bonding is used frequently and increasingly in MEMS technology which requires complex and intricate structures such as the MIT micro-engine which requires 6 or more silicon wafers bonded to each other [4]. Micro-scale combusters, heat exchangers and rocket engines have also made use of bonding. For some applications, especially electronic applications where electric properties are important, it is necessary to be able to bond at low temperature, often lower than the annealing temperature of the substrate, which requires a different procedure to produce, such as bonding without water molecules on the surface [5].

2.1.2 Glass Bonding

Methods other than Fusion Bonding

Apart from fusion bonding, which was the focus of this project, there are also other bonds in existence which are used. These are briefly talked about below, followed by a more extensive review of the literature surrounding fusion bonds.

Anodic bonding is a process which usually bonds a silicon wafer to a glass substrate by placing them between two electrodes and subsequently heating to annealing temperature.

The electrodes provide a DC potential difference up to 1kV and this potential difference causes sodium ions to clean the surface of the glass and cause the silicon's surface to react with the glass surface, forming a bond. It is also possible to use this process to create a glass-glass bond [2].

Plasma bonding involves temporarily cleaning the surface in order to make it hydrophilic, allowing for easier bonding, as is elaborated on in the "Fusion Bonding Chemistry" section. Plasma cleaning uses a machine in order to treat a surface with various gases in order to clean and sterilise it by creating an electric field [6]. The process removes organic contaminants, sterilises the surface and generates hydroxyl groups on the surface if these are not already present.

Bonding using adhesives is the more traditional method of bonding glass substrates. Many different adhesives exist for different applications. Super glue, which sometimes requires a surface activator, can be applied straight to the surface. Epoxy is made up of two parts which need to be mixed prior to application, while cyanoacrylate requires spinning of the surface and applying a daub at the center [2].

Methods of Fusion Bonding

The main process that separates one fusion bonding method from another is the surface preparation (cleaning procedure). In this project, the aim was to test different fusion bonds while only varying the cleaning procedure, while keeping the other variables as constant as possible. Other factors apart from the cleaning/preparation that could have influenced the results include changing the material, varying the annealing procedure from sample to sample and varying the time submerged in each chemical from sample to sample. In this section, different possible cleaning procedures to be used in this project will be looked at, and these will also be treated as the main factor defining a single so-called "fusion bonding method". It should also be noted that leading up to this project, there were several cleaning procedures which 'accompanied' the project in that the intention of trying them was already present going into the project. All the cleans to try during the project were not, however, set in stone so it is important to look at some journal papers in order to get more ideas for possible cleans to try.

The authors of the paper "Sub-60 nm Nanofluidic Channels Fabricated by Glass-Glass Bonding" for example, who bonded glass to glass, as was done in this project, cleaned their samples using an acetone solution, followed by a Piranha bath and subsequently a rinsing in deionised water. The samples were then blown with nitrogen gas and placed in the oven [7]. The authors of "Fabrication of sub-40 nm nanofluidic channels using thin glass-glass bonding" used the same technique to clean their glass [3]. The advantage of this is that the acetone will melt any residual plastics off the samples and the Piranha solution will be relatively successful in burning organics off, but perhaps not as thorough as if a solution with Hydrochloric Acid was used. The rinsing in deionised water and the drying with a nitrogen gun help in ensuring the surface is free of any dust particles and

Piranha residual traces.

The paper "Wafer direct bonding: tailoring adhesion between brittle materials" suggests the Hydrochlric Acid solution at a ratio of 1:1:6 ($HCl:H_2O_2:H_2O$) and an Ammonium Hydroxide Solution at a ratio of 1:1:5 ($NH_4OH:H_2O_2:H_2O$) [8]. It also suggests Piranha at ratios of 1:4 or 1:2 instead of 1:3 (H_2O_2:Sulphuric Acid) as well as a mixture of Hydrogen Peroxide and Nitric Acid [8]. This paper does, however, focus on bonding of silicon rather than glass, so not all these cleaning procedures will necessarily work with glass substrates.

Another cleaning procedure suggested in "Nanofluidic device for continuous multiparameter quality assurance of biologics", where the authors cleaned the samples using a Piranha solution, rinsed with deionised water, and subseqeuntly used 29% NH_4OH to treat the samples for 30 minutes at room temperature, which is different to the ammonium hydroxide solution presented previously [9]. The Hydrochloric Acid only may be better or may be worse at removing organic materials from the glass slides' surfaces than the HCl solution presented previously and eventually used in this project.

In "Capillary kinetics of ferrofluid in hydrophilic microscope slide nanochannels", the authors are also etching and subseqeuntly bonding glass for the purpose of creating nanochannels and in this paper they use Acetone in order to remove any remaining photoresist following the etching process. After this the authors used a HCl solution in order to remove precipitated particles and also, interestingly, to "enhance surface flatness" which is something [8] does not mention as a benefit of using a HCl solution [10]. After this, the authors of [10] used used Piranha solution as the final cleaning step prior to placing the samples in the oven. The amount of influence the removal of organics and other surface 'dirt' has on bond strength and the amount of influence flatness of the glass pieces has will be discussed in the results section, when correlations can be drawn between bond strength and other parameters, such as the area of each bond.

2.2 Glass

2.2.1 Bulk Chemistry

Glass can come in many different types of modified forms in order to give it certain properties, but the form that was used in this experiment was a flat glass, called soda-lime glass, made up mostly of amorphous SiO_2 and with tetrahedra composed of one Si atom connected to four O atoms as the base unit [11]. This base unit can be seen in Figure 2.1 below, with the bond lengths shown.

Silicon Dioxide can be in crystalline or amorphous form. The form most relevant for this project is, obviously, the amorphous form, glass. While both are made of tetrahedral base units, the structure in glass is random, as can be seen in Figure 2.2 [13]. The bond lengths shown in the Figure 2.1 (0.162nm between Si and O, and 0.262nm between O and O) are relatively similar throughout all forms of SiO_2. In fact, glass has the molecule configuration of a fluid (a random configuration) rather than a solid, but due to its extremely high viscosity and covalent bonds between molecules, it exhibits traits of a solid more than of a fluid. Figure 2.2 below compares the chemical structures of

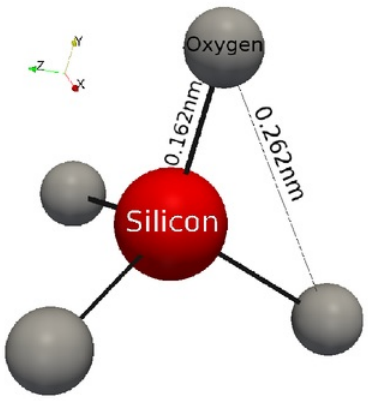

Figure 2.1: The basic bulding block of glass, the SiO_4 tretrahedron [12].

crystalline and amourphous silica. It should be noted that in Figure 2.2 (A) and (B), the image is 2-dimensional, and hence one Oxygen atom connected to each Silicon atom is obscured into the page.

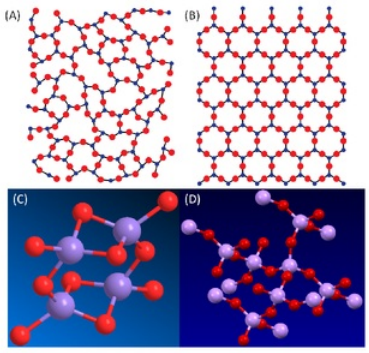

Figure 2.2: Chemical Structure of Silica: In (A) and (B) the Si atoms are blue and the O atoms red, and the fourth O atom is obscured into the page, while in (C) and (D) the Si atoms are purple and the O atoms red. (A) Amorphous SiO_2 [14], (B) Crystalline SiO_2 [14], (C) Amorphous SiO_2 and (D) Crystalline SiO_2.

It should be noted that the basic building block of SiO_2, the SiO_4 tetahedron from 2.1 has its atoms bonded to each other by covalent bonds. Covalent bonds usually exist between atoms of elements relatively close to each other on the periodic table (similar electronegativity). Since Silicon and Oxygen are relatively close on the periodic table (Oxygen has atomic number 8 and Silicon atomic number 14), covalent bonds result between these two elements. Covalent bonds occur when two atoms share a valence electron, as depicted in Figure 2.3 below [11].

Figure 2.3: A covalent bond between two Hydrogen atoms due to sharing of electrons [11].

There is a rule called the octet rule, which states that atoms 'want' 8 electrons in an atom's outer shell (valence electrons) [15]. This means that in the case of glass, Oxygen, since it has six valence electrons, needs two more to obtain eight, and hence obtains two by sharing two with Silicon atoms through covalent bonds. Likewise, Silicon has four valence electrons and needs four more to obtain 8, which it obtains by forming covalent bonds with four Oxygen atoms. Therefore, in Silicon Dioxide, as already mentioned, each Silicon atom is bound to four Oxygen atoms and each Oxygen atoms to two Silicon atoms.

It should be noted that the glass used in this experiment was not pure SiO_2, but so-called 'extra white soda lime glass'. This glass was composed of the following:

- 72.20% SiO_2
- 14.30% Na_2O
- 1.20% K_2O
- 6.40% CaO
- 4.30% MgO
- 1.20% Al_2O_3
- 0.03% Fe_2O_3
- 0.30% SO_3 [16].

This composition might mean that the surface chemistry may not always be that described in the next section and may have a minor effect on the bonding, but since the glass is still predominantly Silicon Dioxide, the bulk and surface-chemistries described here still mostly apply.

2.2.2 Surface Chemistry

The surface chemistry of glass is highly dependent on how many $Si - O - H$ (also called silanol groups) are present on the surface. As can be deduced from the the previous section on the chemistry of bulk glass, the outer atoms of each tetrahedra are Oxygen atoms, as the Silicon atoms are in the middle. However, in a practical sense, unless the hydroxyl groups are purposely removed, the surface of silicon dioxide, and hence glass, usually contains such silanol groups, with Hydrogen atoms on the outside, as can be

seen in Figure 2.4 below. Figure 2.4 does not imply that the Silicon atoms are never in tetrahedra and connected to four Oxygen atoms. Tetrahedra share adjacent atoms to make the overall ration between Si and O 1 : 2.

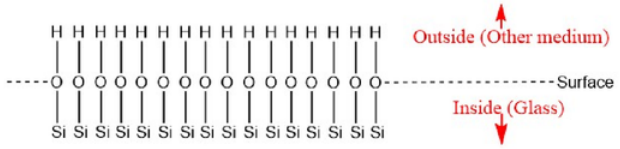

Figure 2.4: The surface chemistry of glass; silanol groups (Silicon, Oxygen and Hydrogen).

These silanol groups can be formed on the surface of SiO_2 (silicic acid) in two ways. Firstly, they can be formed during the process known as silica synthesis, when condensation polymerisation of $Si(OH)_4$ occurs. Condensation polymerisation of $Si(OH)_4$ is a process during which single silicic acid tatrahedra with hydroxl groups connected to the silion atom fuse together to form xerogel, a polymer which retains silanol groups on the surface but not in between the Silicon Dioxide tatrahedra [17]. This process happens during the formation of silica, when silica in its natural form, quartz sand, is melted down and the water molecules (Two Hydrogen and one Oxygen atom) are eliminated, the same way in which they diffuse away during the annealing process of fusion bonds, leaving only one Oxygen atom covalently bonded to two adjacent Silicon atoms. This process can be seen in Figure 2.5 below, where silanol groups are only retained in the xerogel. These hydroxyl and silanol groups on the surface of the glass are the reason the surface is hydrophilic, which is crucial to the bonding process, as is explained later in the 'Bonding Chemistry' section.

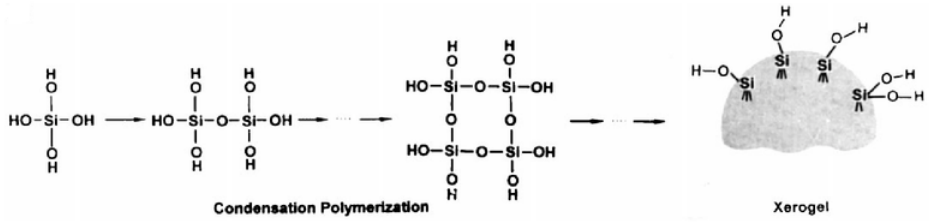

Figure 2.5: The process of condensation polymerisation of $Si(OH)_4$, where individual SiO_2 tetrahedra get fused together and retain hydroxyl groups [17].

The second process which can cause silanol groups to be formed on the surface of SiO_2 occurs when water or other aqueous solutions are applied to the surface of SiO_2. This process is known as rehydroxylation of dehydroxylated silica and when the surface Si-O groups come into contact with H_2O, the free valence of the surface Silicon atoms attract Oxygen atoms from the H_2O and form hydroxl groups at the Silicon atoms where

previously one Oxygen atom was shared between two Silicon atoms [17]. This process can be seen in Figure 2.6 below.

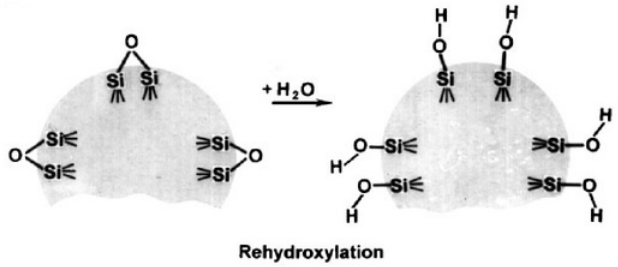

Figure 2.6: The process of rehydroxylation at the surface of SiO_2, where the adding of water causes hydroxyl groups to bond to Silicon atoms [17].

There are several different forms the silanol groups on the surface can take. These can be seen in Figure 2.7.

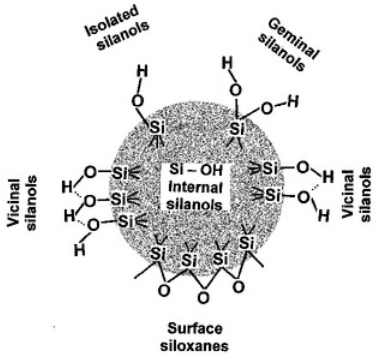

Figure 2.7: The strucures silanols at the surface of SiO_2 can have [17].

In regards to the bonds connecting the Si and O atoms, these are covalent, while the bonds between the O and H atoms are also bonded via a covalent bond. However, the hydroxyl groups on the surface are connected to each other via a hydrogen bond (and dipole-to-dipole forces, which will be explained shortly), which is a secondary bond (compared to the primary covalent bond), and hence much weaker [11]. Figure 2.8 below shows the hydrogen bonds (dotted lines) as well as the covalent bonds (solid lines) which are present on the surface of SiO_2.

A hydrogen bond is a bond which occurs only between molecules which contain covalently bonded Hydrogen and Fluorine (H-F), Hydrogen and Oxygen (H-O, as in the case of glass) and Hydrogen and Nitrogen (H-N) [11]. Hydrogen bonds exist due to the single electron of the hydrogen atom being shared with the other atom (F, O, or N, in this case

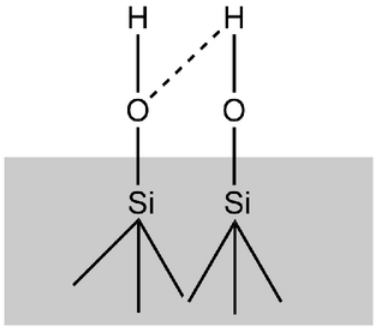

Figure 2.8: The covalent bonds (solid lines) and hydrogen bonds (dotted lines) present on the surface of SiO_2.

the O atom) and hence the Hydrogen atom of the molecule carrying a strong positive charge as the proton of the hydrogen atom is exposed and not screened by any electrons. This strong positive charge can be attracted to a neighbouring molecule's negative side, creating a hydrogen bond, as is shown in Figure 2.9 below for two H-F molecules.

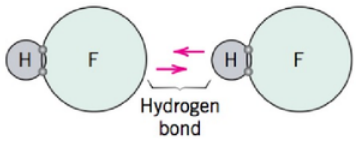

Figure 2.9: A Hydrogen bond between two H-F molecules [11].

These hydroxyl groups on the surface are important as they determine how hydrophilic or hydrophobic (attracted to or repulsed by water, respectively) the surface becomes. If hydroxyl groups exist in sufficient numbers on the surface, the surface is hydrophilic due to a hydrogen bond forming between the Oxygen atoms of the water molecule and the Hydrogen atoms of the surface's hydroxyl groups [17]. This is shown below in Figure 2.10. As well as this, there is also a dipole-to-dipole force acting in unison with the hydrogen bond.

H_2O molecules and hydroxyl groups on the surface of the glass both have a permanent polarity [18]. This means that as well as a hydrogen bond between the hydroxyl groups and the water molecules, there is also a dipole-to-dipole force working to attract the two to each other, as dipole-to-dipole forces occur between molecules which have a permanent polarity [15]. These dipole to dipole forces occur because molecules with a permanent polarity have a tendency to align themselves with their negative end facing the positive end of a neighbouring molecule, creating an electrostatic attraction between the two. From now on, all solid lines in pictures will symbolise covalent bonds and dotted lines will symbolise hydrogen and dipole-to-dipole forces acting in unison.

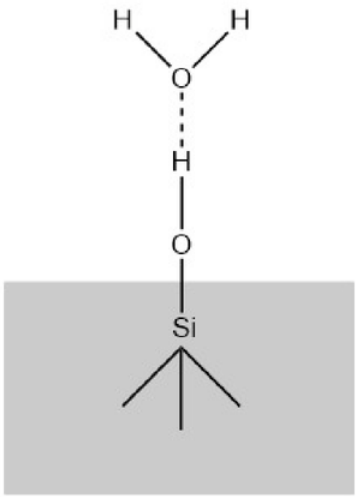

Figure 2.10: The H_2O molecule connected via a hydrogen bond and a dipole-to-dipole force (dotted line) to the surface Hydrogen atom of SiO_2, making the surface hydrophilic.

What has been described above is the molecular surface chemistry that takes place on a perfectly clean piece of glass, with no outside influence. In reality, of course, this is not the case and the surface becomes contaminated with different substances, hence why it is necessary to clean the surfaces. This contamination will be discussed here. This contamination of SiO_2 falls under either particle contamination, organic contamination, or ionic contamination [8]. Particle contamination involves physical particles such as dust or fibres on the surface, while organic contamination refers to substances like hydrocarbons from the air or from finger grease. Ionic contamination refers to metal ions contaminating the surface, originating from eg. metal tweezers. The most significant impact of these three stems from particle contamination, as a particle trapped inside the bond will prevent the bond forming where the particle is, with a non-bonded area much larger than the particle itself. In this project, a clean room was used as well as a Nitrogen gun and an ethanol rub in order to minimise (and ideally, eliminate) the particles on the surface of the glass pieces being bonded. Organic contamination is weaker in its effect as it has little influence on surface roughness and is readily removed with chemical cleans, hence not preventing bonding at room temperature [8]. It can however, limit adhesion between the two surfaces during annealing due to the 'nucleation of interface bubbles', which is why in this project, the Piranha and HCl solutions were used in order to minimise organic contamination, the latter also helping to remove metal ions. Ionic contamination is perhaps the least problematic of the three, as it neither affects the bond at room temperature or during annealing, and may only really be influential when the bond is used for electronic applications as the properties of semiconducter materials such as silicon may be altered through metallic ions. Figure 2.11 below shows the different types of surface

contamination possible during fusion bonding.

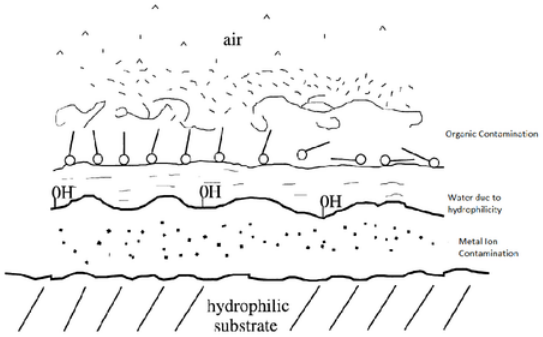

Figure 2.11: The different types of contamination that can occur on the surface of SiO_2; paticle, organic and ionic [8].

2.2.3 Fusion Bonding Chemistry

As discussed in the previous section, the surface of the glass consists of Silanol groups on the surface, which are connected to water molecules through hydrogen bonds and dipole-to-dipole forces, making them very hydrophilic. To understand fusion bonding we must ask, what happens when the two glass surfaces, both covered in water molecules, are pressed together and subsequently heated (almost) to annealing temperature: the answer involves several different types of bonding as well as the process of dissolving of water molecules.

The scenario on each surface immediately before the two glass slides are bonded can be seen in Figure 2.10 on the previous page. When the two surfaces are pressed together, the water molecules on the one hydrophilic surface will mix with those from the other hydrophilic surface, creating a layer of water between the two surfaces. The water mixes due to hydrogen bonds (and dipole-to-dipole forces) forming between the H_2O molecules. However, since the water here is in a liquid state, these only exist between some molecules, as can be seen in Figure 2.12 below [15].

Therefore, when the two glass surfaces are pressed together, the molecular arrangement looks like that shown in Figure 2.13:

It should be noted here that it is unclear how many layers of water will be formed between the two surfaces. Since the pieces of glass are not perfectly flat, the layers of water between them will be different in different places. Where the two glass slides are sufficiently close together, the annealing process diffuses the water molecules away and subsequently creates a Si-O-Si covalent bond structure between the two glass pieces [5]. This process is the same as was described previously in Figure 2.5 during the condesation polymerisation process, when silicic acid fuses together to become silica. This means that

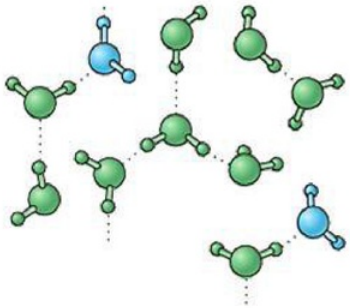

Figure 2.12: Hydrogen bonds (and dipole-to-dipole forces) forming between some, but not between all, molecules in liquid water [15].

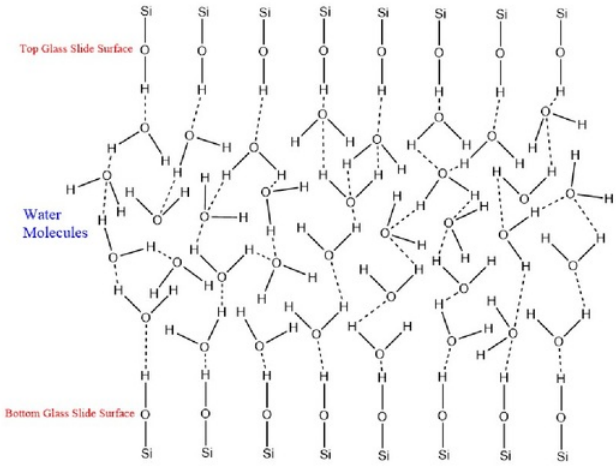

Figure 2.13: The reversible bond between the two glass surfaces formed prior to any annealing.

where this happens, there will no longer be a water layer or any sort of boundary between the layers, and the glass pieces will become one piece. This can be seen in Figure 2.14 below.

As mentioned above, this fusion as shown in 2.14 does not happen everywhere (only where the glass pieces are sufficiently close together), and in the places where it doesn't there will still be water (and possibly some contaminants) between the glass pieces and the bond will remain reversible, held together only by hydrogen bonds and dipole-to-dipole forces. This is illustrated in Figure 2.15 below.

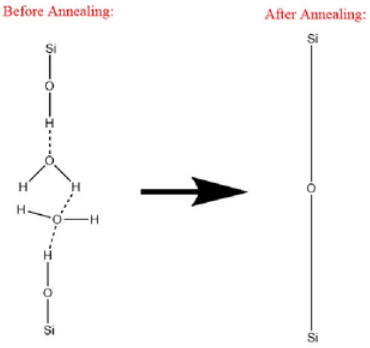

Figure 2.14: The water layer between the two glass surfaces prior to annealing and the fused SiO_2.

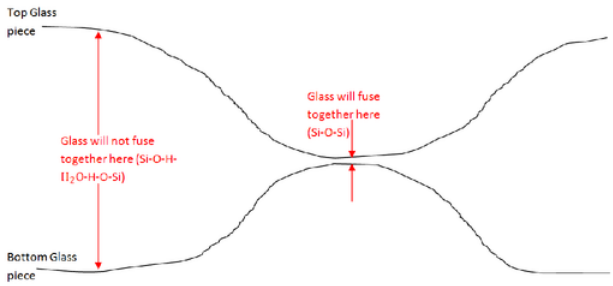

Figure 2.15: The fusion bond (Si-O-Si) will form at peaks on the glass surface where the surfaces are sufficiently close together.

2.3 Mechanical Testing

2.3.1 Stress and Strain Theory

The standard type of test for testing material properties is the tensile test, where a sample of a certain material is pulled apart at both ends until fracture [11]. Figure 2.16 below shows the stadard force that is applied along the axis of the sample for a tensile test.

The equation below is used to calculate the stress from the force applied and the displacement of the material before fracture.

$$\sigma = \frac{F}{A_0} \tag{2.1}$$

where σ is the stress (Pa), F the force (N) and A_0 the cross-sectional area of the glass slide (m^2). It should be noted that A_0 is always the area under stress, so in the tests with the bonded samples, A_0 will be the bonded area, while for a single glass slide, it would

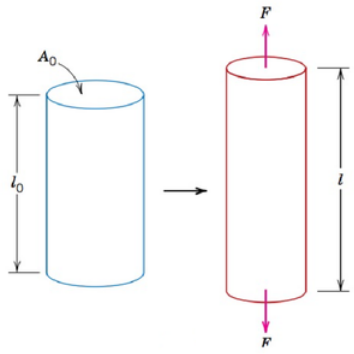

Figure 2.16: The force applied perpendicular to the cross-sectional area and outwards in order to perform a standard tensile test on a single material [11].

be the cross-sectional area.

The strain can also be calculated using the equation below.

$$\epsilon = \frac{\Delta l}{l_o} \tag{2.2}$$

where ϵ is the strain (unitless), Δ the displacement, or change in original length (m) and l_o the original length of the sample (m). The strain can also be calculated if the stress and Young's Modulus of a material are known, using the equation below:

$$\epsilon = \frac{\sigma}{E} \tag{2.3}$$

where ϵ is the strain, σ the stress (Pa) and E the Young's Modulus (Pa).

In terms of this project, most tests were slightly more complicated, although the same principles still applied. Firstly, the tests conducted were compression tests, which are similar to tensile tests, except for the fact that the force applied is inward, towards the sample's centre, and not outward. This can be seen in Figure 2.17.

As well as this, the test in this project applied a shear force as the force was parallel to the area under stress (the bonded area), rather than a normal force. An illustration of what a shear force on a single block of material looks like can be seen in Figure 2.18.

While the equations are virtually the same for calculating stress and strain for a shear force than a normal force, it is important to differentiate between a shear force and a normal force, and hence different letters are used in the equations below.

$$T = \frac{F}{A_0} \tag{2.4}$$

$$\Upsilon = \frac{\Delta l}{l_o} \tag{2.5}$$

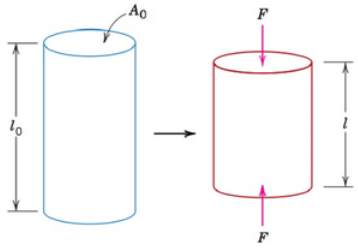

Figure 2.17: The force applied perpendicular to the cross-sectional area and inwards in order to perform a standard compression test on a single material [11].

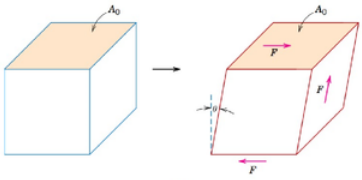

Figure 2.18: The force applied parallel to the area under stress to achieve a shear force [11].

where T is the shear stress and Υ is the shear strain (unitless).

Regardless of whether the type of force applied is a normal or a shear force, a stress-strain graph is generally used to convey the information, as it neutralises area under stress that was used. A typical stress-strain graph for a ductile material, as can be seen in Figure bla bla below, contains a section where the material deforms elastically (if force is removed it will return to its original shape), which is the straight-lined, left-most part of the graph. The end of this line is the Yield Stress of a material, which is the maximum stress at which the material will spring back to its original shape if the force is removed [11]. The gradient of this line is also the Young's Modulus. Next, after the elastic deformation line there is a curved, concave down line, where the material plastically deforms (changes shape irrevesibly), but the force being applied continues to increase. When the highest point of this line is reached and the slope of the line's tangent starts to become negative, the Tensile Strength of the material is reached, which is the absolute maximum point a material (or in this case, a bond) can take. Beyond this, the stress decreases again until the material fractures [11]. In terms of this project, the material being tested was brittle, which meant that theoretically, only the elastic part of this curve should exist. Figure 2.19 below shows this for a standard ductile material.

A brittle material such as glass, which was tested in this project, theoretically produces a different kind of stress-strain graph, one with little or no plastic deformation, and only predominantly elastic deformation. This means it breaks shortly after the linear region and the yield strength is equal to the tensile strength. This can be seen in Figure

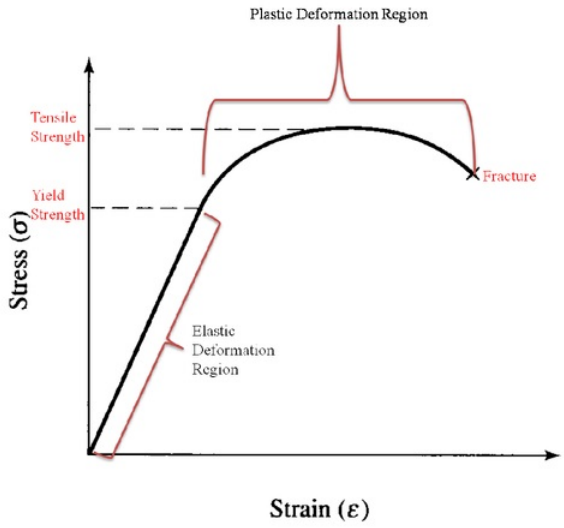

Figure 2.19: How a stress-strain curve of a ductile material looks in theory.

2.20 below, a ductile and a brittle material's stress-strain graphs are compared, with the subscript 'f' denoting the point of fracture.

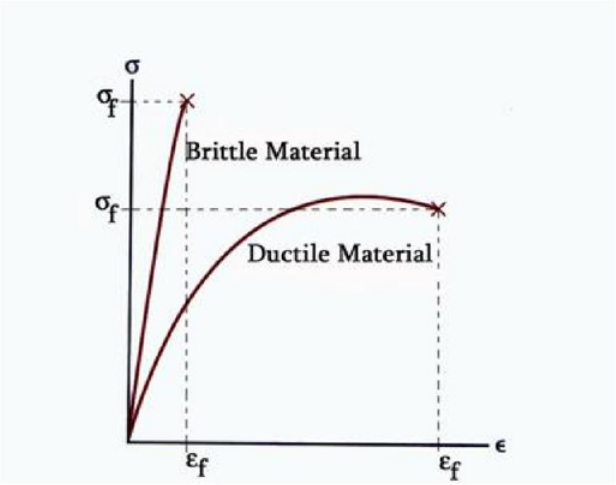

Figure 2.20: A typical brittle material's theoretical stress-strain graph, with little to no corvature, compared to a ductile material's graph [19].

It should also be noted that in this project, since a piece of aluminium was glued directly to the glass sample, the sample's Modulus of Rigidity ($\frac{\text{ShearStress}}{\text{ShearStrain}}$) may have been altered slightly. However, since the Modulus of Rigidity of both these materials is very similar (around 29 MPa), this influence was minimal. The main reason the aluminium plates were used was because aluminium is a ductile material while glass is a very brittle material, and thus the joining of the two prevented premature cracking. As well as this, the tensile strength of aluminium is also larger than that of glass, meaning that by reinforcing the parts of the sample which were not the desired fracture points, the bonded area was made the weakest point of the sample, making the sample much more likely to fracture there.

2.3.2 Bond Testing Methods

Another major question that needed to be addressed during this project is how exactly the strength of the bonds would be tested. A few ideas had been thrown around which included three-point flex testing, as well as normal tensile testing with varying degrees of overlap (bond surface area) between the two pieces of materials. In this section, the bond testing methods conducted in some journal papers will be examined.

The journal paper entitled "Plastic-Silicon Bonding for MEMS Packaging Application" examines the strength of a silicon-plastic bond with the help of tensile testing and the use of a strong adhesive [20]. This paper uses normal tensile testing with the bond being tested angled perpendicular to the pulling direction. It also utilises a strong adhesive (stronger than the bond being tested) to attach the two sides of the bond to materials which can be pulled on by the tensile testing machine. This can be seen in Figure 2.21. This tensile testing procedure may not be applicable in this project due to a glass-glass bond being made, and glass being a much more brittle material than plastic and silicon, meaning it is weak under tension due to cracks propagating more easily. A different testing method is introduced in the journal paper entitled "Bonding of polymer and glass using nano-adhesion layer for flexible electronics", where a testing method called T-peeling is used in order to get an idea of the bond's strength [21]. This is done by seeing whether the sample peels away at the bond or at the bulk of one of one of the material slabs. The disadvantage of this method compared to the method in [20] is that it only gives one a rough idea of the bond strength in relation to whether it is stronger or weaker than the bulk material, and not a yield strength, tensile strength, etc. in terms of quantitative pressure. This may make it unsuitable for this project but a similar variant of it will likely still be attempted en route to finding the most suitable testing method for this project.

The method used for bond testing in "Investigation of various photo-patternable adhesive materials and their processing conditions for MEMS sensor wafer bonding" not only quantifies pressure, but also has the added advantage of avoiding any clamping (and hence, possible premature breakage of sample) by simply gluing the sample to the jaws using an adhesive, as in [20], where an adhesive is used that is stronger than the bond [22] Due to glass being a very brittle material, clamping of the sample may mean an undesirable force on the sample which can cause it to crack prior to the testing taking

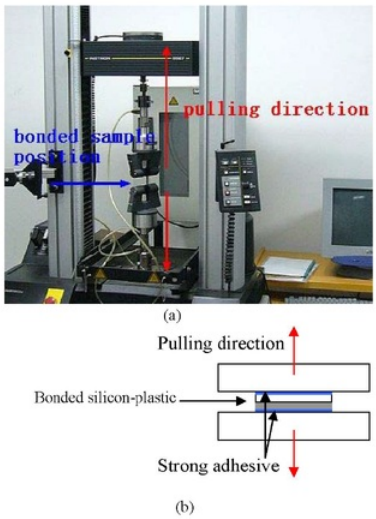

Figure 2.21: The tensile testing method used in order to test the bond [20].

place. The paper "Interface Adhesion Between Copper Lead frame and Epoxy Moulding Compound: Effects of Surface Finish, Oxidation and Dimples", which tested the bond strength between a molding compound and a copper lead frame, utilised the services of a tensile testing machine as well, pulling the bond apart in order to create a force [23]. The paper [24] is interesting in its approach to testing here because it is testing two glass pieces which are connected, albeit not directly as in this experiment. In [24], the authors use a compression test to create a shear force, something which is good for glass due to its higher strength under compression. Here they create a double shear force instead of a single shear force (as would be done in this project due to the two glass pieces being directly bonded) so it is a little different, but the same principle would still apply. The testing procedure can be seen in Figure 2.22 below.

2.3.3 Results presentation

Now that it is clear what stress and strain is and how it is calculated, a brief discussion should be made in regards to how the results should be presented. The results will be given in the form of a stress-strain graph for each sample, but how will the different types of fusion bonds be compared? It is important to present the results clearly and as easily understandable as possible.

The journal paper [25], "Determining the optimal PDMSPDMS bonding technique for microfluidic devices", does this well as it gives a range for each cleaning procedure's stress and strain. Since in this project two samples of each cleaning procedure were tested, it would be possible to calculate the maximum, minimum, and average maximum shear stresses and present them in a graph as can be seen in Figure 2.23 below.

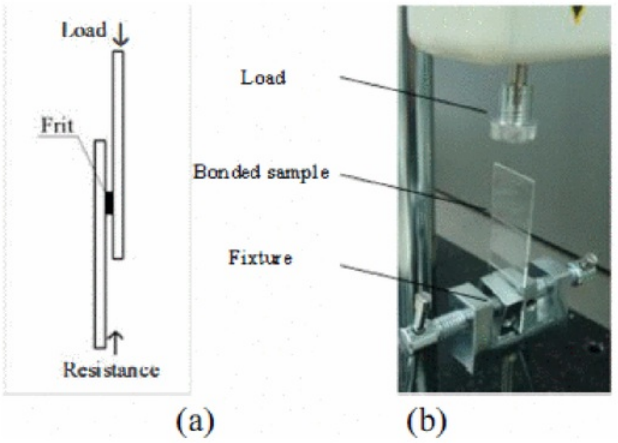

Figure 2.22: Testing of Bonded Samples: (a) Diagram of shear force test, (b) shear force test setup for bonded sample [24].

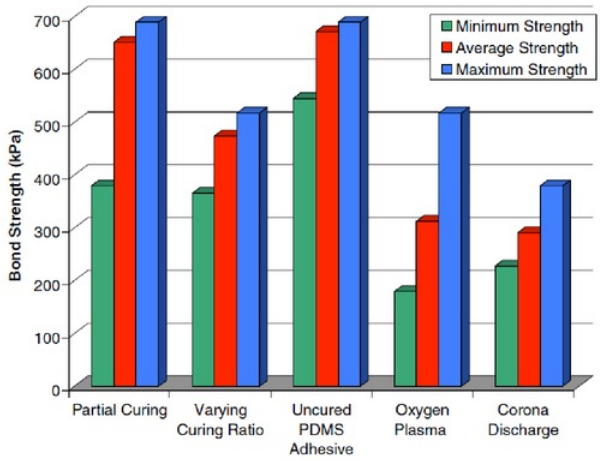

Figure 2.23: The minimum, maximum, and average stresses for each set of conditions, similar to what will be displayed in this project [25].

It is also possible to present the results in the form of a chart which gives the range as a single bar, where the bottom of the bar represents the minimum and the top presents the maximum, as was done in "Mechanical strength and interface characteristics of glass-to-glass laser bonding using glass frit" [24]. "Effects of surface roughness and oxide layer on wafer bonding strength using transmission laser bonding technique"' presents the results in a useful way as it considers several parameters in one graph (Figure 2.24), which may

be useful for this project, as the contact pressure may have been different, due to some bonds bonding instantly and some bonds needing pressing by hand [26]. This, however, is difficult to quantify so it may not be possible to consider it in the result section, as well as maybe not being completely relevant either, as all that matters is that the sample bonded, not how.

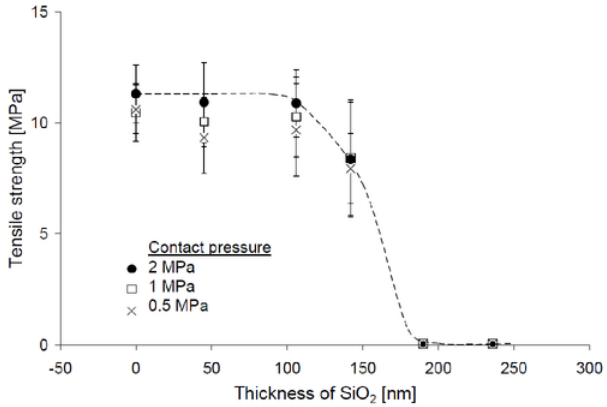

Figure 2.24: This graph takes into account three factors: contact pressure, SiO_2 thickness (constant in this project) and tensile strength [26].

Chapter 3

Methodology

This section will describe the procedure that was used in order to perform this experiment from the creation of the bonds to the processing of the results.

Firstly, pieces of glass had to be fusion bonded. This was done in a clean room, where the amount of particles in the air was roughly 1000 per cubic meter, as opposed to the 10^9 found in regular air, on average. The aim with this was to minimise the possibility of particles coming in between the two bonded surfaces. As explained in the previous chapter, physical particles such as hair or dust have the greatest chance of jeoperdising bond creation at room temperature. As well as the clean room, a nitrogen gun was used in order to blow any particles off the surface of the glass following the cleaning step, immediately before bonding.

The bonding process itself involved some different procedures, as the cleaning procedure was the independent variable in the expirement. The cleaning procedures that were used were:

- Ethanol Rub - The surface of the glass was rubbed with a cloth soaked in ethanol for about 30 seconds, sprayed with a Nitrogen gun, rinsed in deionised water, and sprayed with the nitrogen gun again, before being pressed together.
- Ethanol Rub + NH_4OH - The ethanol rub was performed as previously described, but additionally the sample was given a bath in a solution composed of 5 parts deionised water, one part Ammonium Hydroxide (NH_4OH) and one part Hydrogen Peroxide (H_2O_2) for about five minutes. The surfaces were then rinsed in deionised water, dried with the nitrogen gun and pressed together to form a bond. This clean was done due to not having to use Piranha or Hydrochloric Acid, which were the two most dangerous solutions used in the four cleans for this experiment.
- Piranha + NH_4OH - The samples were given a 5 minute bath in Piranha solution, which is composed of three parts Sulfuric Acid and one part Hydrogen Peroxide. Subsequently, the samples were rinsed in deionised water and given a bath in the same Ammonium Hydroxide solution detailed above. The samples were then rinsed in deionised water again and dried with a nitrogen gun before being pressed together to form a bond.

- Piranha + HCl + NH_4OH - The samples were given a 5 minute bath in Piranha solution, rinsed with deionised water, then given a 5 minute bath in Hydrochloric Acid solution, which was made up of 6 parts deionised water, one part Hydrochloric Acid (HCl) and one part Hydrogen Peroxide. They were then rinsed again and finally given a bath in the NH_4OH solution described previously. Then, they were rinsed a final time, dried with a Nitrogen gun, and pressed together to form a bond.

It should be noted that for these cleans, the ethanol rub was done at room temperature, while the Ammonium Hydroxide and Hydrochloric Acid solutions were heated to 75°C prior to the samples being immersed in them. The Piranha solution would bubble for a while after first being mixed and only when this bubbling subsided was it heated to 50°C. The dishes with the solutions inside were covered in glass lids to preserve the chemical reactions as much as possible. The process was done in a fume hood in order to avoid inhalation of chemical fumes, and while working with chemicals a face shield, double gloves and thick plastic apron were worn to avoid skin or eye contact with any chemicals. The setup inside the fume hood with all three chemical solutions (Piranha, Hydrochloric Acid and Ammonium Hydroxide) can be seen in Figure 3.1 below.

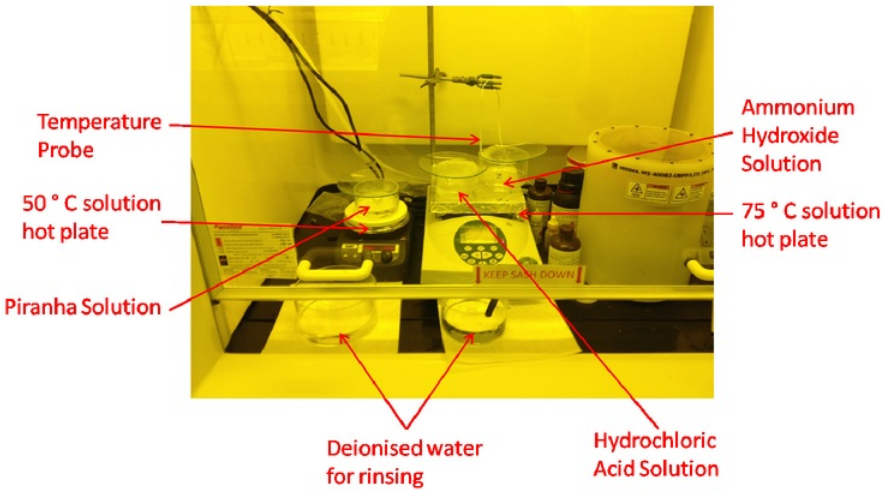

Figure 3.1: Experimental setup when cleaning glass with chemicals. It should be noted that the hot plates were hotter than 75 and 50°C, this was just the temperature of the solution.

After the samples had been bonded reversibly at room temperature, it was time to put them in the oven. Every effort was made to place them in the oven as quickly as possibly following bonding at room temperature as the bond in some cases would start coming apart as long as it was still reversible. Once placed in the oven, the temperature would be raised to 400°C at a rate of 3°C/min, held at 400°C for 10 hours and then allowed to cool.

The sample was usually placed in the oven one day and taken out the next. Once this was done, the samples were labelled and the sample number, cleaning procedure, overlapping area and bonded area were recorded. The labelling was done on the frost which was part of the glass slides as can be seen below in Figure 3.2.

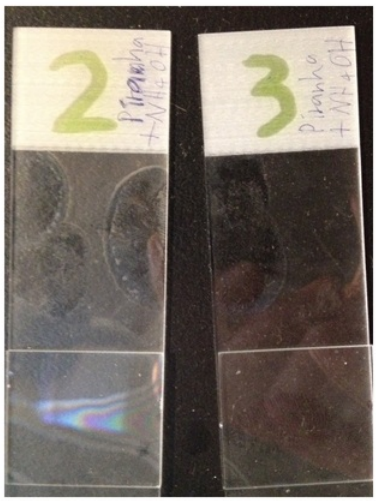

Figure 3.2: Labelling of samples. This was the sample number recorded in order to identify each sample's properties.

While the overlapping area could be measured with a ruler, the bonded area had an irregular shape and was not so simple to measure with a ruler. In order to obtain this quantity, a program called 'Image J' was utilised in order to process an image of the bond. A picture was taken of the sample against a dark background so it was clear where the bonded area (no newton lines visible) and the non-bonded area (newton lines visible) were. The program then allowed for the measurement of the bonded area by counting pixels after a scale had been manually set. This can be seen in Figure 3.3 below.

After the samples were ready and documented, it was time to test them. The most obvious way to test a sample is a normal tensile test. This was tried with several different configurations but ultimately failed due to the glass simply being too brittle and it being extremely difficult to have it fracture at the bonded area. Figure 3.4 below shows several different configurations which were tried out.

The hard rubber did not absorb the pressure of the clamps very well and hence the force of them was transferred onto the glass sample, cracking it before the sample was fully clamped. The clamps were designed for metal samples which they would bite into so it was difficult to use them on a glass sample due to it being so much more brittle than any metal. The cardboard did a better job of absorbing the force but it would slip as the adhesion between it, the glue and the glass sample was not very strong. The sticky, soft rubber double-sided tape worked the best and absorbed all the force from the clamping,

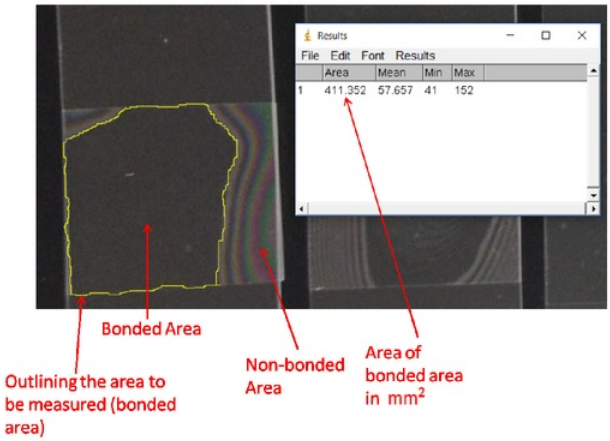

Figure 3.3: The processing of the image on Image J and measuring the bonded area of the sample.

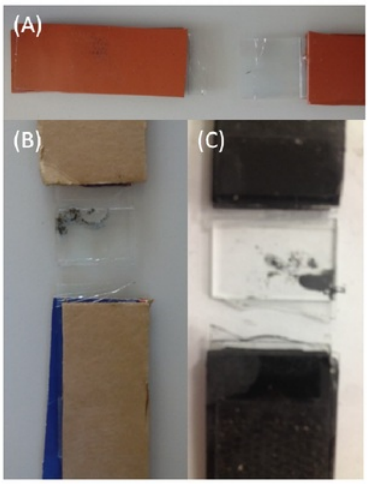

Figure 3.4: Failed Tensile Testing Methods: (A) Hard rubber, (B) Cardboard and (C) Sticky soft rubber double-sided tape.

but the sample would often break during clamping and despite it breaking in the correct spot, this was still not a working testing method.

Another method that was tried was the T-Peeling method, where two samples were crossed over each other and bonded in the middle. The aim was to use a three-point testing configuration in order to bend the sample and peel away at the bond. This did not work however, as the glass was not elastic enough to peel away at the bond, and one

piece of the glass would just break, as can be seen in Figure bla bla below.

Figure 3.5: Breakage of sample following peeling test attempt on a glued sample.

Following this, a working method was finally come up with in the form of a compression test. The tensile testing machine had two compression plates designed in order to perform compression tests on blocks of material such as concrete. This process was modified by making two aluminium plates, one which could be screwed to the top compression plate and one with an L-shape which could be rested to the bottom compression plate or fitted to it with a clamp. Then, the sample was glued to both these using super glue and the compression test commenced until the sample broke at the bonded area. This can be seen in the diagram and photo in Figure 3.6 below.

In order to re-use the aluminium plates for subsequent samples, the two aluminium plates (now with glass glued onto them from the broken sample) were soaked for 20-30 minutes in Acetone which caused the glue to melt and allowed the glass to be chiseled off. The tensile testing machine produced a Force vs. Displacement graph and excel data, which was converted into the Stress vs. Strain graph which can be seen for each sample in the results section. This process was repeated until three samples of each cleaning procedure had been produced and tested.

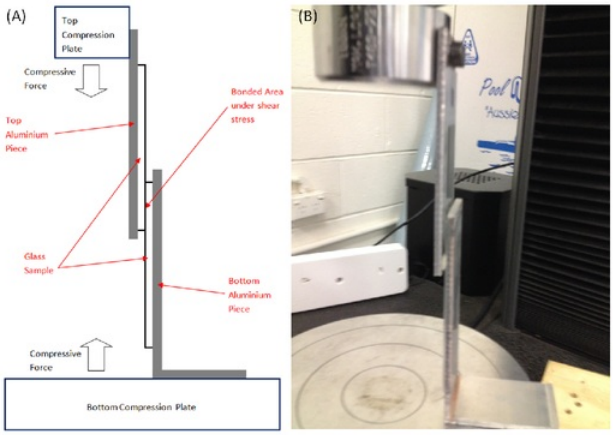

Figure 3.6: Testing method involving the compression plates: (A) Diagram and (B) Photo.

Chapter 4

Results

4.1 Table of Samples

This chapter presents the results of the testing of the bonds. The first table gives some details on each sample, while graphs show the data from each test. An "N/A" in cells for the 'Bonded Area (Estimate)' column and in some cells for the 'Overlapping Area' column indicates it was unnecessary to measure these areas for the samples that broke (prior to testing or during testing but in the wrong place), and only the samples which were successfully tested are guaranteed to have all quantities.

Sample Number	**Cleaning Procedure**	**Overlapping Area**	**Bonded Area (Estimate)**	**Result**
1	Ethanol	702mm^2	N/A	Broke
2	Piranha + NH_4OH	N/A	N/A	Broke
3	Piranha + NH_4OH	N/A	N/A	Broke
4	Ethanol + NH_4OH	N/A	N/A	Broke
5	Piranha + HCl + NH_4OH	390mm^2	386mm^2	Broke
6	Ethanol	625mm^2	N/A	Broke
7	Ethanol	550mm^2	N/A	Broke
8	Ethanol	500mm^2	N/A	Broke
9	Ethanol	546mm^2	N/A	Broke
10	Ethanol	520mm^2	345mm^2	Tested
11	Ethanol	438mm^2	129mm^2	Tested
12	Ethanol + NH_4OH	497mm^2	364mm^2	Tested
13	Piranha + HCl + NH_4OH	500mm^2	101mm^2	Tested
14	Piranha + HCl + NH_4OH	475mm^2	291mm^2	Tested
15	Piranha + NH_4OH	663mm^2	383mm^2	Tested
16	Piranha + NH_4OH	463mm^2	275mm^2	Tested
17	Piranha + NH_4OH	700mm^2	411mm^2	Not Tested
18	Ethanol + NH_4OH	500mm^2	452mm^2	Tested

19	Ethanol + NH_4OH	574mm^2	528mm^2	Not Tested
20	Ethanol + NH_4OH	463mm^2	428mm^2	Not Tested
21	Ethanol + NH_4OH	481mm^2	204mm^2	Tested
22	Piranha + HCl + NH_4OH	497mm^2	133mm^2	Tested
23	Piranha + HCl + NH_4OH	488mm^2	474mm^2	Not Tested
24	Piranha + NH_4OH	488mm^2	452mm^2	Not Tested
25	Ethanol	536mm^2	307mm^2	Tested
26	Ethanol + NH_4OH	446mm^2	452mm^2	Tested

Table 4.1: List of all bonded samples that were created.

4.2 Regular Glass Slide Tests

Figure 4.1 shows the testing results of a regular glass slide. The machine's output provided time elapsed, displacement and Force applied. These were converted to shear stress and strain using 2.1 and 2.2 the cross-sectional area of the glass slide (26mm^2) and the length of the glass slides (76mm).

The results in Figure 4.1 above are as expected. Glass is a brittle material and therefore there is little or no plastic deformation when it is tensile or compression tested, meaning that the curve should theoretically be a straight line until breakage. Figure 4.1 is almost a straight line, except for perhaps a slight curve that is concave down. Also, the maximum stress for the compression test is much higher than that of the tensile test, which is also expected as tension encourages cracks in a brittle material to propagate by pulling them apart, while compression tends to push them together, making it harder for them to propagate. According to [11], the tensile strength is about double (69 MPa) of what the compression test results yielded.

Figure 4.1 (B)s test was different to that in Figure 4.1 (A) in that it was a compression test rather than a tension test meaning that the outputs given by the machine were the time elapsed (s), the displacement (mm) and the force, but this was given in kgf rather than Newtons.

4.3 Sample 10 (Ethanol Rub)

Figure 4.2 below shows Sample 10's Stress-Strain graph as well as the sample after the breakage. The shear stress and strain had to be calculated using equations 2.4 and 2.5, and subsequently the two could be graphed.

Figure 4.3 below shows the same data as Figure 4.2, except that this stress-strain graph has been adjusted for slippage/slack at the start. This sort of slippage/slack is present all throughout the raw data from the tensile testing machine and it could have

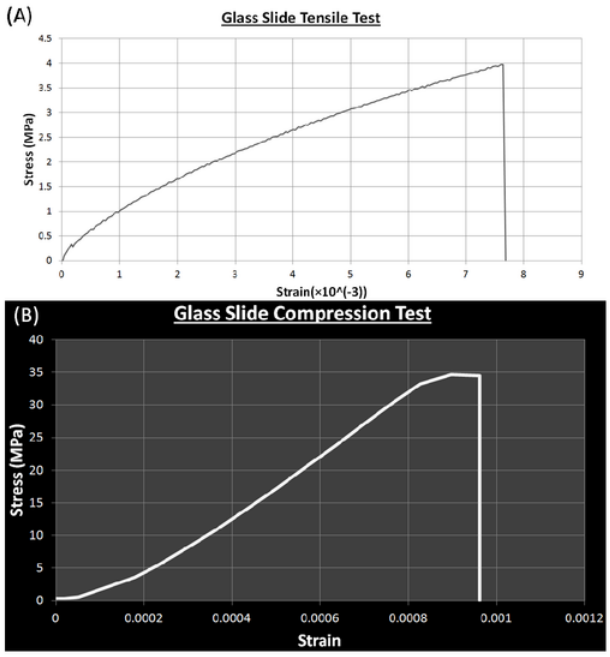

Figure 4.1: Test results for a regular glass slide: (A) Tensile Test and (B) Compression Test

occurred because the machine had some force acting on the compression plate initially due to gravity, or because there was a slight distance between the bottom aluminium piece used for testing and the compression plate it was resting against. This graph has been made for every sample and is the data that will be used to compare samples and cleaning procedures with each other, as it most accurately reflects the data from the test of the sample and excludes as many external factors as possible.

What can be seen in Figure 4.3 is that between the strains of roughly 0.001 and 0.004 the stress-strain curve has an unexpected shape in that it looks almost like the $y = x^3$ curve when $x < 0$ and $y < 0$. This shape is unexpected, as the stress-strain graph for a brittle material should be roughly straight, as there is little or no plastic deformation occuring, and only the straight curve from the elastic deformation up until the yield strength (where fracture occurs) is visible. The shape in Figure 4.3 between the strains 0.001 and 0.004 means that the sample was being pushed apart while the rate of compressive force application was decreasing. This could possibly be due to the sample cracking below or above the bond, and the shear force pushing this crack apart after it had already propagated, leaving less resistance than usual, causing the rate of force increase to decrease, while the tensile testing machine kept the rate of extension constant. Then, once this crack has been pushed apart but other areas around the bond have not cracked

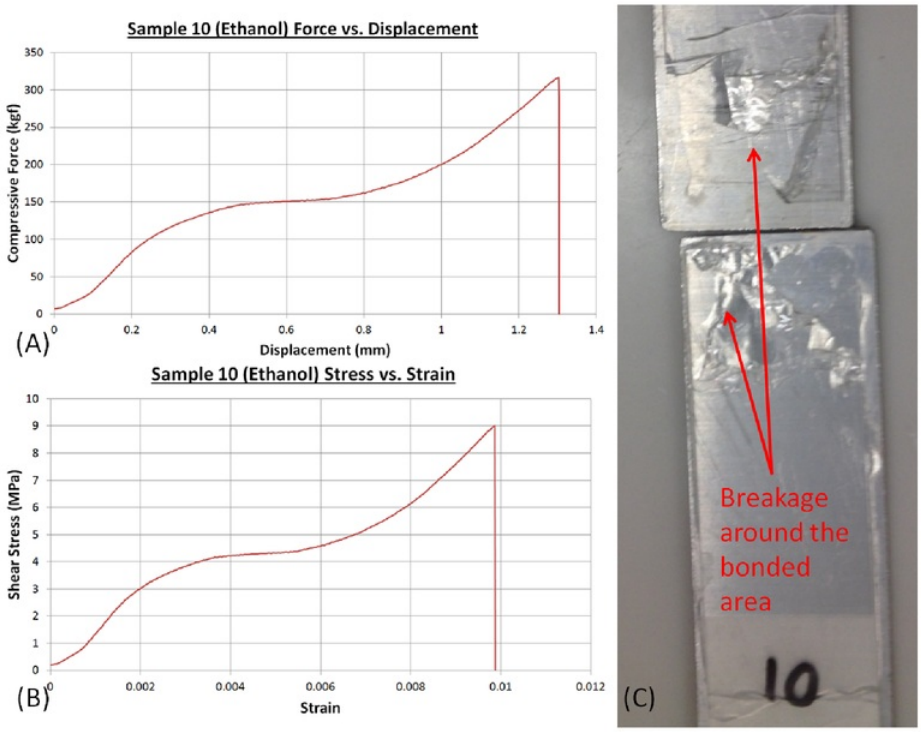

Figure 4.2: Compression test results for Sample 10: (A) The original force vs. displacement results from the tensile testing machine. (B) The results when converted into a stress vs. strain graph. (C) Sample 10 after it broke under the compression test.

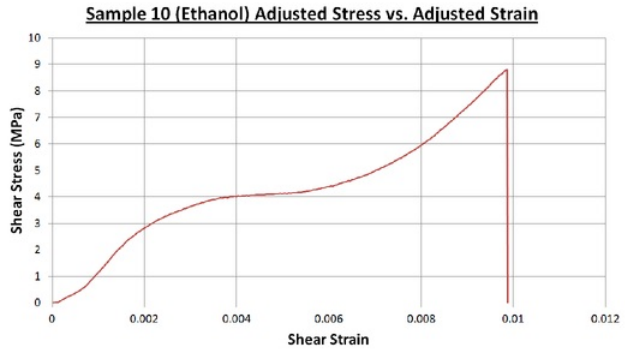

Figure 4.3: The stress vs. strain graph from Sample 10 adjusted for initial inaccuracies.

yet, the normal force required to keep the rate of extension of the sample constant will resume, and the curve takes back a more normal shape as can be seen in Figure 4.3 when the strain is > 0.004. For all the following samples, such deviations from the norm of a brittle material's stress-strain curve were likely due to this, or due to the sample cracking a few times in quick succession without completely breaking if some cracking occured permaturely, so the shape of the other curves will not be discussed.

4.4 Sample 11 (Ethanol Rub)

The results for Sample 11 were processed in the same way as those for Sample 10. The original force vs. displacement graph given as the output by the tensile testing machine was shown, and subsequently the stress and strain of was calculated from these two quantities. Figure 4.4 below shows the original results of Sample 11's breakage, as well as the adjusted stress vs. strain graph. The process for arriving at the stress vs. strain graph seen in part (C) of Figure 4.4 was the same with every sample so for subsequent samples only these graphs will be displayed, as these contain the maximum shear stress which will be used at the end to compare not only the samples of the same cleaning procedures, but also of different cleaning procedures.

Figure 4.5 below compares the before and after images of Sample 11. As with Figure 4.4, this will not be displayed in subsequent samples, as the breakages looked similar for every result, with the sample fracturing roughly around the bonded area, but not exactly.

The graph which can be seen from Figure 4.4 is relatively devoid of any abnormalities as far as the expected results are concerned.

4.5 Sample 12 (Ethanol Rub + Ammonium Hydroxide Solution)

The same process was repeated for Sample 12, the results of which can be seen in figure 4.6 below. As mentioned before, from this sample onwards, only the finalised, adjusted, stress vs. strain graphs will be shown as the process undertaken to reach it was already shown and is the same for every sample.

4.6 Sample 13 (Piranha + Hydrochloric Acid Solution + Ammonium Hydroxide Solution)

Sample 13, the results for which can be seen in Figure 4.7 below, was cleaned using first Piranha Solution, then HCl solution and subsequently an NH_4OH bath. The graph did not have to be adjusted for initial slack or slippage as the gradient at $(0, 0)$ already started increasingly appropriately, and there was minimal initial force due to the weight of the top compression plate.

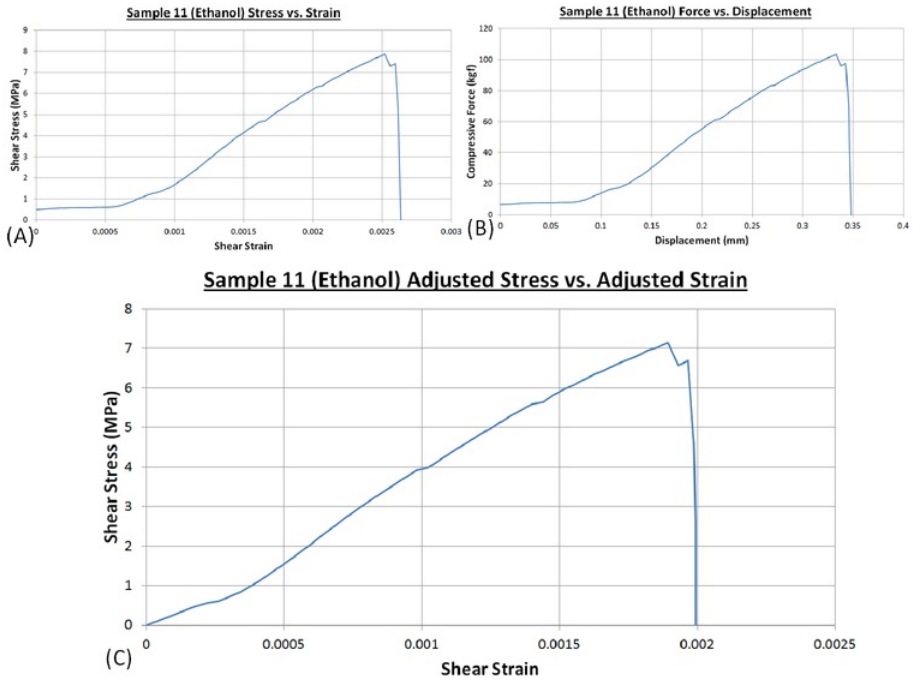

Figure 4.4: Compression test results for Sample 11: (A) The stress vs. strain curve obtained from the original results. (B) The original force vs. displacement data. (C) The graph from (A), but adjusted for initial slack/slippage.

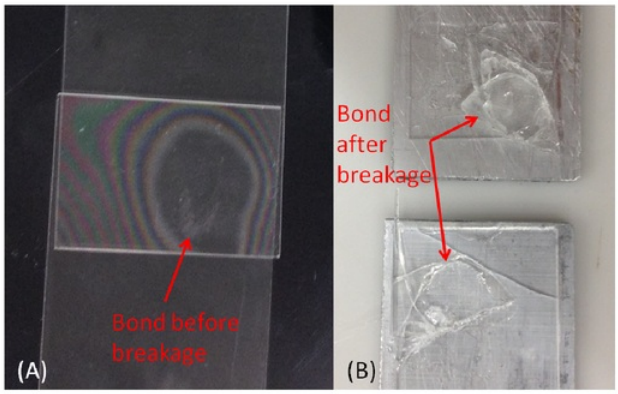

Figure 4.5: Sample 11 before and after: (A) Sample 11 prior to fracture. (B) Sample 11 after fracture.

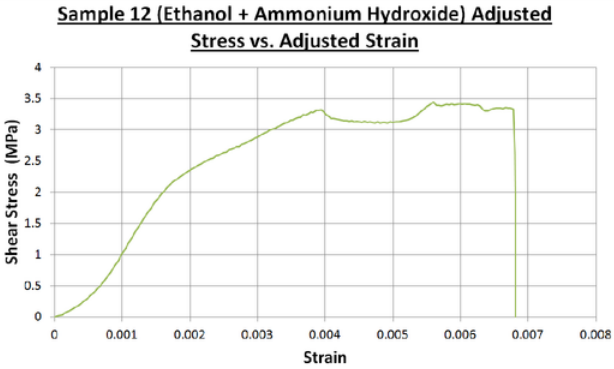

Figure 4.6: The results obtained from the compression test of Sample 12.

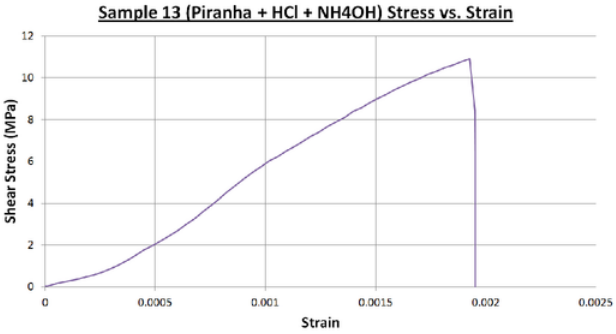

Figure 4.7: The resulting stress vs. strain graph for Sample 13.

4.7 Sample 14 (Piranha + Hydrochloric Acid Solution + Ammonium Hydroxide Solution)

The graph below in Figure 4.8 is the result of Sample 14's compression test. The graph did not need to be adjusted for any initial slack or slippage.

4.8 Sample 15 (Piranha + Ammonium Hydroxide Solution)

Figure 4.9 below shows the results of Sample 15's test, which was cleaned using Piranha and subsequently an Ammonium Hydroxide Solution.

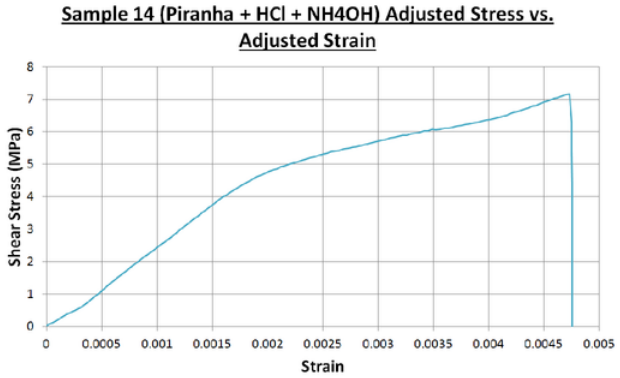

Figure 4.8: The resulting stress vs. strain graph for Sample 14.

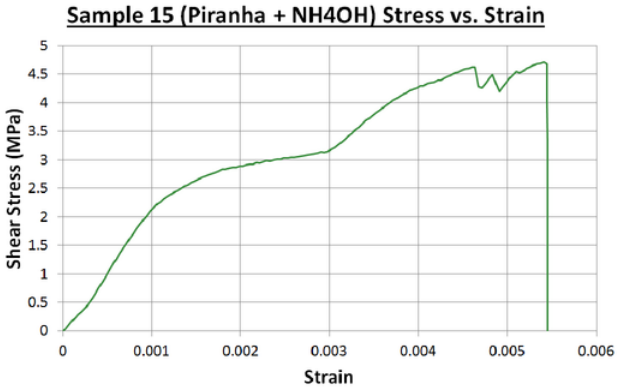

Figure 4.9: The resulting stress vs. strain graph for Sample 15.

4.9 Sample 16 (Piranha + Ammonium Hydroxide Solution)

Below, in Figure 4.10, the results from Sample 16's compression test can be seen.

4.10 Sample 21 (Ethanol Rub + Ammonium Hydroxide Solution)

Figure 4.11 below shows the results obtained from Sample 21.

The noticeable kink in the graph between the strains of 0.01 and 0.04 is due to a crack propagating through the middle of the sample (but not causing it to break prematurely). This was observed during the test. The sample still fractured in the correct place.

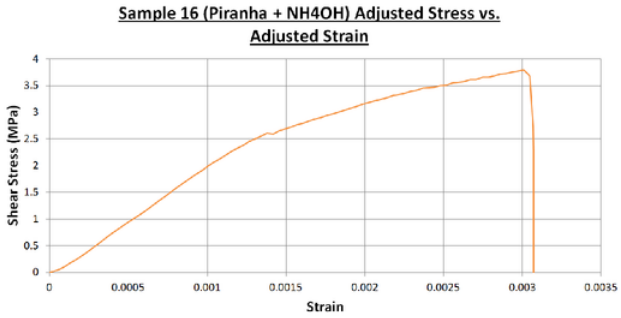

Figure 4.10: The resulting stress vs. strain graph for Sample 16.

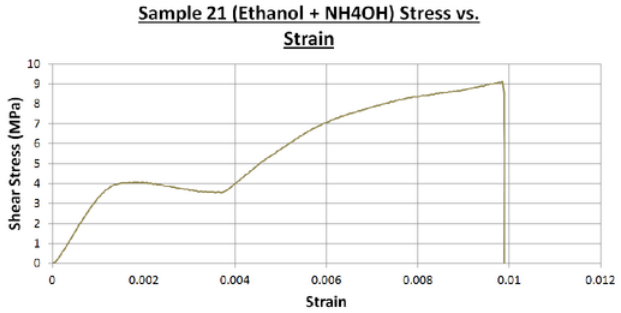

Figure 4.11: The resulting stress vs. strain graph for Sample 21.

4.11 Sample 22 (Piranha + Hydrochloric Acid Solution + Ammonium Hydroxide Solution)

The graph in Figure 4.12 below is the stress-strain graph for Sample 22.

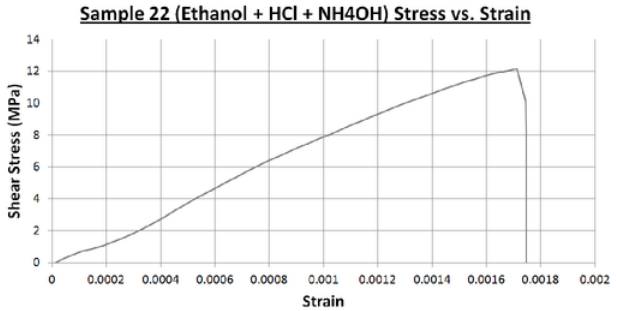

Figure 4.12: The resulting stress vs. strain graph for Sample 22.

There is nothing unusual or unexpected about the shape of the graph in Figure 4.12.

4.12 Sample 25 (Ethanol Rub)

The graph in Figure 4.13 below shows the stress-strain curve for Sample 25.

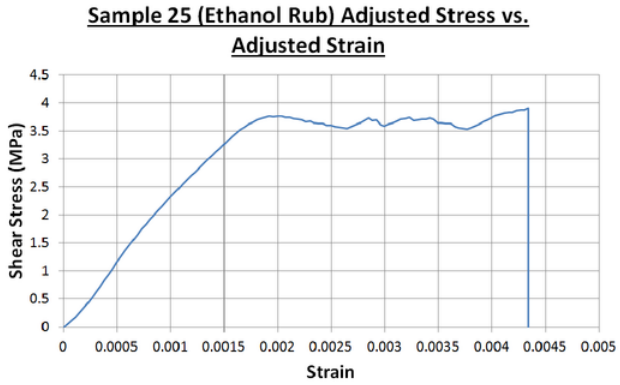

Figure 4.13: The resulting stress vs. strain graph for Sample 25.

4.13 Sample 26 (Ethanol + Ammonium Hydroxide Solution)

The graph below in Figure 4.14 shows the result of Sample 26's test.

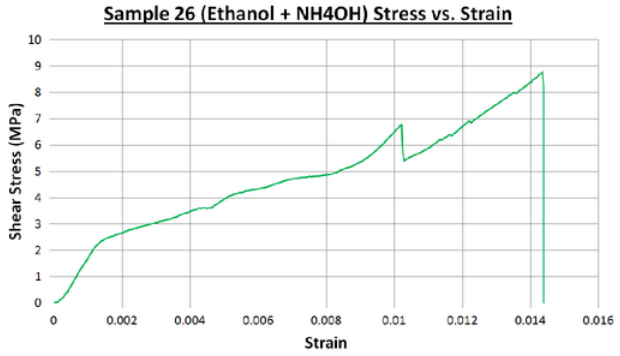

Figure 4.14: The resulting stress vs. strain graph for Sample 26.

4.14 Glued Sample Compression Test

Figure 4.15 shows the results when a glued sample (using super glue) was tested using the same procedure as the bonded samples.

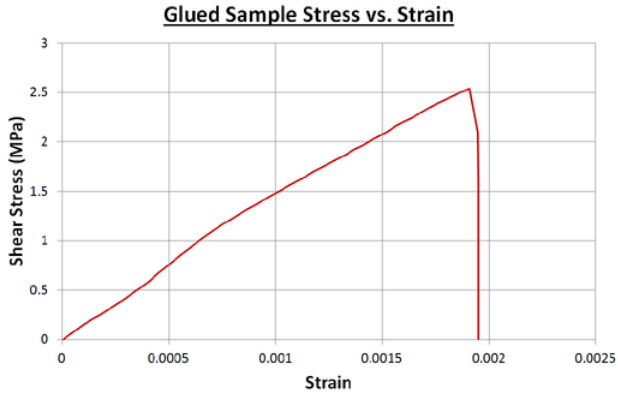

Figure 4.15: The resulting stress vs. strain graph of the glued sample.

4.15 Comparison between cleaning procedures

The purpose of the figures below is to compare the stress-strain graphs firstly between two of the same cleaning procedures and secondly across all the cleaning procedures. Figure 4.16 below shows the variation between the maximum stress of Sample 10, 11 and 25, which were all cleaned using an ethanol rub.

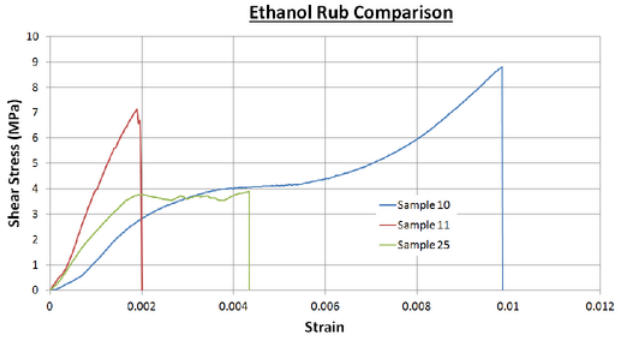

Figure 4.16: Comparison between the maximum shear stresses of Samples 10, 11 and 25.

Figure 4.17 shows the difference between the three samples which were cleaned using Piranha, Hydrochloric Acid solution as well as Ammonium Hydroxide solution.

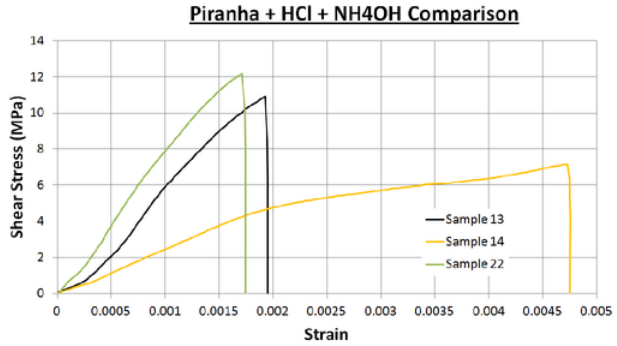

Figure 4.17: Comparison between the maximum shear stresses of Samples 13, 14 and 22.

Figure 4.18 compares the three samples prepared with Piranha solution and Ammonium Hydroxide Solution, which were both prepared using Piranha Solution and Ammonium Hydroxide Solution.

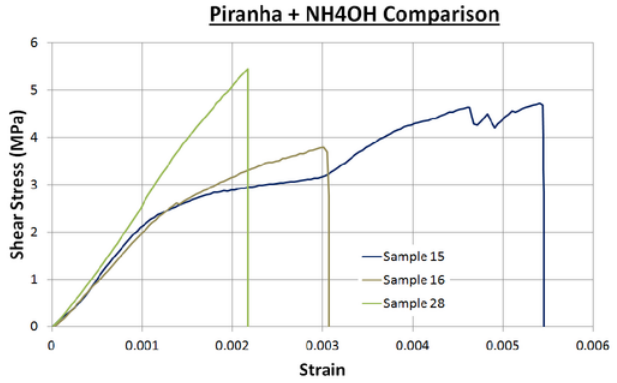

Figure 4.18: Comparison between the maximum shear stresses of Samples 15, 16 and 28.

Finally, Figure 4.19 compares the stress-strain graphs of the samples prepared using an ethanol rub and a bath in Ammonium Hydroxide Solution.

The figures above, which compare the stress-strain graphs of the same cleaning procedures to each other on the same set of axes, provide two important pieces of information per graph. Firstly, it can be seen from each of the graphs how great the difference between the maximum shear stresses (the peaks) is, and secondly it can be seen how great the

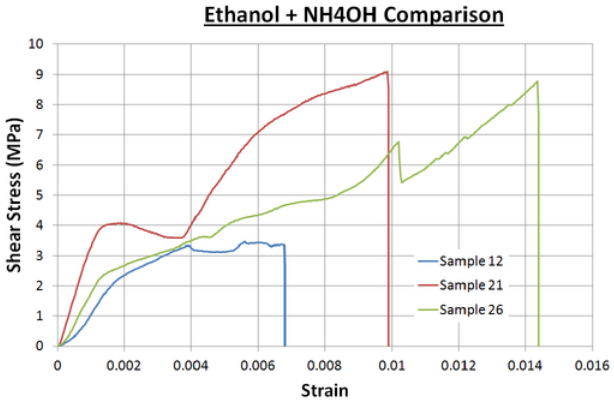

Figure 4.19: Comparison between the maximum shear stresses of Samples 12, 21 and 26.

strain difference is. The maximum shear stresses in the graphs are relatively close to each other except perhaps in Figure 4.17, where it is larger. The two tables below show these two important pieces of information.

Sample Number	Cleaning Procedure	Max. Shear Stress	Corresponding Strain	Bonded Area
10	Ethanol	8.808 MPa	0.009867	345 mm^2
11	Ethanol	7.142 MPa	0.001892	129 mm^2
25	Ethanol	3.896 MPa	0.004345	307 mm^2
12	Ethanol + NH_4OH	3.448 MPa	0.005605	364 mm^2
21	Ethanol + NH_4OH	9.100 MPa	0.009849	204 mm^2
26	Ethanol + NH_4OH	8.774 MPa	0.014358	452 mm^2
13	Piranha + HCl + NH_4OH	10.91 MPa	0.001926	101 mm^2
14	Piranha + HCl + NH_4OH	7.160 MPa	0.004734	291 mm^2
22	Piranha + HCl + NH_4OH	12.16 MPa	0.001712	133 mm^2
15	Piranha + NH_4OH	4.711 MPa	0.005408	383 mm^2
16	Piranha + NH_4OH	3.793 MPa	0.003009	275 mm^2
28	Piranha + NH_4OH	5.445 MPa	0.002174	242 mm^2

Table 4.2: List of all samples successfully tested.

What can be deduced from the table above is that the different strains for the samples are roughly proportional to the bonded areas of the samples. The smaller the bonded area of a sample, the smaller the strain is at the maximum shear stress. This could be due to several factors, such as the crack having to propagate further, as the perimeter around the bonded area is bigger, and hence the sample "slipping" a little before fully coming apart. Also, a similar phenomenon could be taking place, but rather than slipping parallel to the direction in which the tensile testing machine is applying compressive force, the sample could be cracking and the compressive forces be out of alignment slightly, resulting in a small torque being applied, which would increase the strain prior to the sample fully breaking.

Figure 4.20 compares the different cleaning procedures side-by-side according to maximum shear stress.

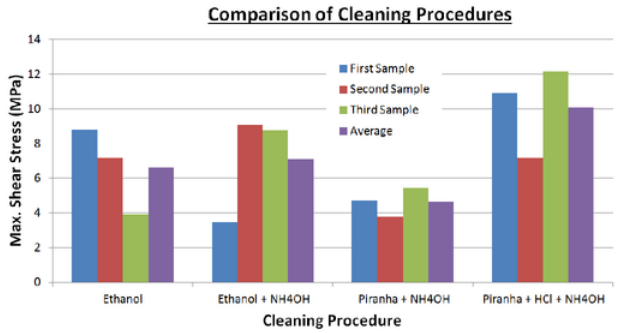

Figure 4.20: Comparison across all tested cleaning procedures.

Figure 4.21 summarises the final results of the experiment, comparing the average maximum shear stresses for each cleaning procedure from 4.20, as well as a sample bonded with super glue.

4.16 Analysis & Discussion of Results

In this project, every effort was taken in order to keep as many variables as possible constant. These included re-using the same aluminium plates for every sample tested, using the exact same model of glass slide for every sample created, using the exact same oven for every sample, and using the same procedure to clean glass slides for each clean. Despite this, there are still outliers in the results. These and other inaccuracies could be due to many factors, including the aluminium plates being at a slightly different angle to the compression plates during each test, the top aluminium plate being slightly loose, the super glue holding the sample to the plates slipping slightly during the compression test or the bonded area not being measured 100% accurately. These inaccuracies could be

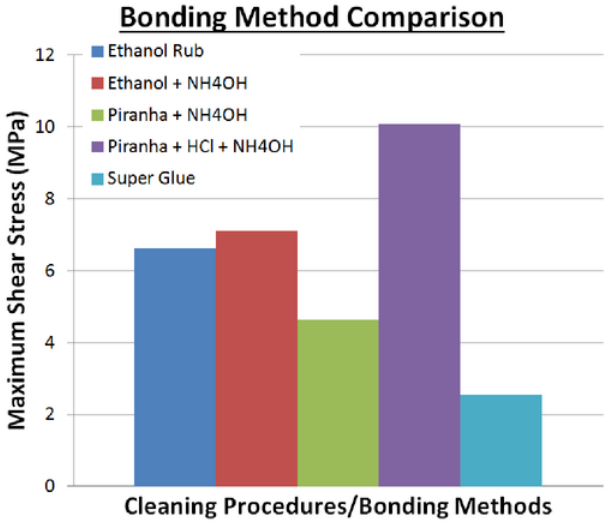

Figure 4.21: Comparison across methods of bonding tested in this experiment.

further minimised by performing more tests per cleaning procedure and hence obtaining more data points to average.
This experiment could not, of course, cover every investigative aspect of fusion bonding, and like any other experiment, has some limitations. The first major limitation of this project was that only regular, soda-lime glass slides were used for the bonding process. Coming into the project, the intention was to test multiple cleaning procedures as well as multiple variations of Silicon Dioxide if time permitted, including quartz and pure amorphous Silicon Dioxide. This however, was not possible due to the time limitations imposed on the experiment by the time taken to find the right testing method (several weeks out of 13). The second major limitation is that only four different cleaning procedures were tested, while many more (and several variations of those in this experiment) can be found in the literature. The third major limitation of the project was that only hydrophilic surfaces were used for bonding. Fusion bonding of hydrophobic glass substrates also exists and this could have been explored too.
The project's results summarised in Figure 4.21 show that the Piranha, Hydrochloric Acid and Ammonium Hydroxide procedure created the strongest bond, the Ethanol Rub with Ammonium Hydroxide Solution came second, a simple Ethanol Rub was a close third while the Piranha and Ammonium Hydroxide was a relatively distant last, despite still being about twice as strong as using super glue. This was a somewhat different result to that which was expected, as the Ethanol Rub was the most simple one, not requiring any chemicals. It can also be deduced from Figure 4.21 that the Ethanol Rub and Hydrochloric Acid Solution are the single most effective methods of preparing the surface for a bond. This is likely because an ethanol rub is great at removing any particle contam-

ination, while Hydrochloric Acid removes most organics and ionic contamination (even though the latter does not influence the surfaces' ability to form a bond). Therefore, going forward from this project, an ethanol rub followed by a bath in Hydrochloric Acid solution should be used to create and test a bond, in order to potentially create an even stronger bond than any of the ones in this project.
The aim of this project was to find the 'optimal' fusion bond, a term which can encompass more than just the strength of the bond. The two main factors to be considered on top of the strength are safety and cost.

The cost of each of the solutions used is given below, per single use, to make several samples (usually two or three) as used in this experiment. In this project, 100mL of each solution was made, while for the ethanol rub a few squirts were used per sample, meaning that overall, per session in the clean room, about 100mL of ethanol were used (for multiple samples). In order to super glue a sample together, about 1mL of super glue was used, so for a few samples several mL would be used. The price of paper cloths for the ethanol rub was neglected, like the price of deionised water. All the prices for the chemicals as well as the ethanol were taken from the Sigma Aldrich website. The quantities of chemical in the bottles varied and larger bottles were better value, while bulk buying would reduce the price even further, so for industrial applications these prices may well be significantly lower than for individual applications such as this project. Also, the chemical baths can be used to make many samples, without requiring more than the initial 100mL of chemical solution. The ratios between the prices of the different cleans should be relatively similar, however.

- Ethanol Rub - $3.02
- Ethanol Rub + Ammonium Hydroxide Solution - $7.66
- Piranha Solution + Ammonium Hydroxide Solution - $16.27
- Piranha Solution + Hydrochloric Acid Solution + Ammonium Hydroxide Solution - $20.92
- Super Glue - $2.45

The risk level while all the correct safety procedures are followed is relatively low, but below is a list of the relative risk each solution carries with it, in regards to the damage it can do if coming into contact with the human body (In ascending order of risk: Very Low, Low, Medium, High, Very High). The main two chemicals which need to be handled with caution are the Sulfuric Acid and the Hydrogen Peroxide due to the violent reaction these create when contacting any organics.

- Piranha Solution - Very High
- Ammonium Hydroxide Solution - High
- Hydrochloric Acid Solution - High

- Ethanol Rub - Very Low
- Super Glue - Low

Therefore, out of the four cleans tested, the optimal fusion bond as it is relatively strong for how cheap it is and for the low safety risk it carries. The Hydrochloric Acid Solution comes a close second as it provides a major advantage in terms of strength, but is relatively expensive and carries a relatively high safety risk. The other three bonding methods have some major disadvantages; Ethanol and Ammonium Hydroxide Solution carries a high risk for almost negligible gain in strength, while Piranha and Ammonium Hydroxide Solution carries an even higher risk and is weaker, while both are still more expensive than an ethanol rub. Super glue is a good option as long as strength is not the priority. As mentioned previously, moving forward from this project, it could well be that an Ethanol Rub followed by a bath in Hydrochloric Acid Solution, if the results from this project carry into a test of this procedure's strength (it should, theoretically, according to the results from this experiment be stronger than any tested here). Despite still being relatively dangerous, the risk can be minimised greatly by using the correct safety procedure and the strength advantage would outweigh the cost.

4.17 Conclusion

The aim of this project was to find the optimal cleaning procedure for fusion bonding which was accomplished by not only testing the different bonds for their strength but also by considering safety and cost, which resulted in the strongest fusion bond not being the optimal one. Overall, the experiment was a success and despite some problems occurring, especially during testing due to the glass being so brittle, good results were obtained despite these having some outliers. The conclusion drawn at the end was that the strongest fusion bond cleaning procedure is the one using Piranha, Hydrochloric Acid and Ammonium Hydroxide Solution, while the optimal one is a simple ethanol rub due to its low cost and safety risk.

Bibliography

[1] K. Schjlberg-Henriksen, L. G. W. Tvedt, S. Moe, E. Poppe, D. Wang, S. A. Gjelstad, C. Mrk, and K. Imenes, "Bond strength of conductive si-si fusion bonded seals," in *2014 Symposium on Design, Test, Integration and Packaging of MEMS/MOEMS (DTIP)*, April 2014, pp. 1–6.

[2] J. Werkmeister and A. Slocum, "Investigating Different Methods of Bonding Glass Substrates," *Precision Engineering Research Group*, 2010.

[3] Y. K. Lin and J. N. Kuo, "Fabrication of sub-40 nm nanofluidic channels using thin glass-glass bonding," in *2011 6th IEEE International Conference on Nano/Micro Engineered and Molecular Systems*, Feb 2011, pp. 351–354.

[4] A. A. Ayon, X. Zhang, K. Turner, D. Choi, B. Miller, S. Nagle, and S. M. Spearing, "Low temperature silicon wafer bonding for mems applications," in *Technical Digest. MEMS 2002 IEEE International Conference. Fifteenth IEEE International Conference on Micro Electro Mechanical Systems (Cat. No.02CH37266)*, Jan 2002, pp. 411–414.

[5] A. Berthold, B. Jakoby, and M. Vellekoop, "Wafer-to-wafer fusion bonding of oxidized silicon to silicon at low temperatures," *Sensors and Actuators A: Physical*, vol. 68, no. 1, pp. 410 – 413, 1998, eurosensors XI. [Online]. Available: http://www.sciencedirect.com/science/article/pii/S0924424798000284

[6] P. Scientific. Plasma treatment for PDMS, glass slides, lab-on-a-chip and other microfluidics applications. PIE Scientific. [Online]. Available: http://www.piescientific.com/Application_pages/Applications_Microfluidics

[7] K. P. Liao, N. K. Yao, and T. S. Kuo, "Sub-60 nm Nanofluidic Channels Fabricated by Glass-Glass Bonding," in *2006 International Conference of the IEEE Engineering in Medicine and Biology Society*, Aug 2006, pp. 2832–2835.

[8] A. Plößl and G. Kräuter, "Wafer direct bonding: tailoring adhesion between brittle materials," *Materials Science and Engineering*, pp. 1–88, 1999.

[9] J. Han, D. Chandra, W. Ouyang, T. Kwon, P. Karande, and S. H. Ko, "Nanofluidic device for continuous multiparameter quality assurance of biologics," *Nature Nanotechnology*, pp. 1–11, May 2017.

[10] W. K. Wang and J. N. Kuo, "Capillary kinetics of ferrofluid in hydrophilic microscope slide nanochannels," in *The 9th IEEE International Conference on Nano/Micro Engineered and Molecular Systems (NEMS)*, April 2014, pp. 485–489.

[11] W. D. Callister and D. G. Rethwisch, *Materials Science and Engineering*, 9th ed., B. Stenquist, Ed. John Wiley & Sons, 2015.

[12] Silicon Dioxide Properties. imgarcade. [Online]. Available: http://imgarcade.com/silicon-dioxide-structure.html

[13] W. H. Zachariasen, "The Atomic Arrangement In Glass," *Journal of the American Chemical Society*, vol. 54, no. 10, pp. 3841–3851, 1932. [Online]. Available: http://dx.doi.org/10.1021/ja01349a006

[14] T. Husband. (2014, October) The Sweet Science of Candymaking. American Chemical Society. [Online]. Available: https://www.acs.org/content/acs/en/education/resources/highschool/chemmatters/past-issues/archive-2014-2015/candymaking.html

[15] R. Petrucci, G. Herring, J. Madura, and C. Bissonnette, *General Chemistry - Principles and Modern Applications*, 10th ed., L. Campbell, Ed. Pearson Canada, 2011.

[16] (2008) Thermo Scientific Microscope Slides. Gerhard Menzel Glasbearbeitungswerk GmbH & Co KG. Saarbrückener Straße 248, 38116, Braunschweig, Germany. [Online]. Available: https://www.globalcube.net/clients/beldico/content/medias/products/6_imp/labo/disposables/microscopy/slips/menzel_microscope_slides.pdf

[17] L. Zhuravlev, "The surface chemistry of amorphous silica. Zhuravlev model," *Colloids and Surfaces A: Physicochemical and Engineering Aspects*, vol. 173, no. 1, pp. 1 – 38, 2000.

[18] Polar Molecules. Tutor Vista. [Online]. Available: http://chemistry.tutorvista.com/organic-chemistry/polar-molecules.html

[19] Note on Graph of brittle and ductile material. Kullabs.com. [Online]. Available: https://www.kullabs.com/classes/subjects/units/lessons/notes/note-detail/9517

[20] X. Lou, Z. Li, and Y. Jin, "Plastic-Silicon Bonding for MEMS Packaging Application," in *2006 7th International Conference on Electronic Packaging Technology*, Aug 2006, pp. 1–3.

[21] T. Matsumae, M. Fujino, K. Zhang, H. Baumgart, and T. Suga, "Bonding of polymer and glass using nano-adhesion layer for flexible electronics," in *2015 10th International Microsystems, Packaging, Assembly and Circuits Technology Conference (IMPACT)*, Oct 2015, pp. 180–183.

[22] J. Kim, I. Kim, and K. W. Paik, "Investigation of various photo-patternable adhesive materials and their processing conditions for MEMS sensor wafer bonding," in *2011 IEEE 61st Electronic Components and Technology Conference (ECTC)*, May 2011, pp. 1839–1846.

[23] J.-K. Kim, M. Lebbaj, J. H. Liu, J. H. Kim, and M. M. F. Yuen, "Interface adhesion between copper lead frame and epoxy moulding compound: effects of surface finish, oxidation and dimples," in *2000 Proceedings. 50th Electronic Components and Technology Conference (Cat. No.00CH37070)*, 2000, pp. 601–608.

[24] Z. Chen, Y. Lai, L. Yang, and J. Zhang, "Mechanical strength and interface characteristics of glass-to-glass laser bonding using glass frit," in *2012 13th International Conference on Electronic Packaging Technology High Density Packaging*, Aug 2012, pp. 1609–1613.

[25] B. K. G. Mark A Eddings, Michael A Johnson, "Determining the optimal PDMS-PDMS bonding technique for microfluidic devices," *Journal of Micromechanics and Microengineering*, April 2008.

[26] J.-S. P. Tseng, A.A., "Effects of surface roughness and oxide layer on wafer bonding strength using transmission laser bonding technique," *Thermal and Thermomechanical Phenomena in Electronics Systems*, pp. 1349–1357, June 2006.